

Ground State Electronic Interactions in Macrocyclic Fullerene Bis-Adducts Functionalized with Bridging Conjugated Oligomers

Teresa M. Figueira-Duarte,^[a] Vega Lloveras,^[b] José Vidal-Gancedo,^[b]
Béatrice Delavaux-Nicot,^{*[c]} Carine Duhayon,^[c] Jaume Veciana,^{*[b]} Concepció Rovira,^{*[b]}
and Jean-François Nierengarten^{*[a]}

Dedicated to Professor Fritz Vögtle on the occasion of his 70th birthday

Keywords: Fullerenes / Conjugated oligomers / Electrochemistry / π - π interactions

Macrocyclic C₆₀-(π -conjugated oligomer) dyads have been prepared from the corresponding bis-malonates by a macrocyclization reaction on the C₆₀ sphere. In both multicomponent systems, the fullerene moiety and the π -conjugated oligomer subunit are at the van der Waals contact due to the cyclic structure. Interestingly, the characteristic π - π^* electronic transition band of the conjugated system is significantly red-shifted in both dyads with respect to the corresponding model compounds lacking the fullerene unit ($\Delta\lambda_{\max}$ = 24 to 34 nm). Whereas the absorption properties are dramatically affected by the intramolecular electronic interactions between the conjugated bridging system and the ac-

cepting C₆₀ spheroid, cyclic voltammetry revealed only small changes in their redox potentials. However, these intramolecular interactions have a significant influence on the electronic coupling of the two terminal aniline redox units of the conjugated system in the dyads. Actually, when compared to the corresponding model compound **14**⁺, delocalization of the positive charge in the mixed-valence species derived from the dyad **1** is more difficult due to the π - π interactions of the conjugated system with the electron-withdrawing fullerene group.

(© Wiley-VCH Verlag GmbH & Co. KGaA, 69451 Weinheim, Germany, 2009)

Introduction

Hybrid systems combining C₆₀ with π -conjugated oligomers have shown a wide range of physical properties that make them attractive candidates for a variety of interesting applications in materials science.^[1] Indeed, spectacular photoactive systems associating fullerene moieties with π -conjugated donors have been described in the recent past.^[1] Their photophysical properties have been extensively studied.^[2] Whereas the influence of the donating ability of the oligomer unit and of environmental factors such as the

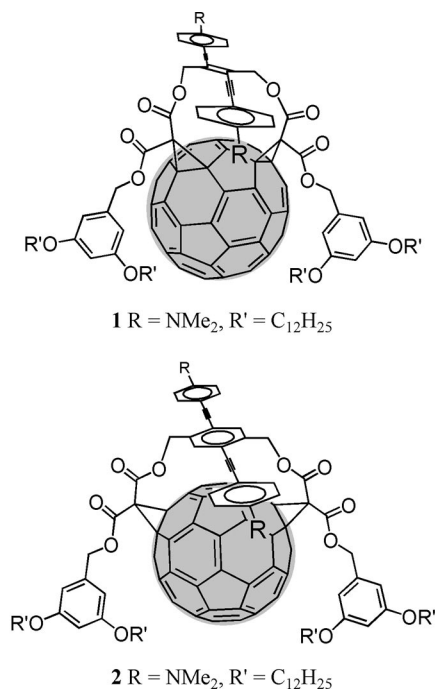
solvent polarity on the deactivation pathways (electron transfer vs. energy transfer) are well established,^[3] the importance of structural factors are not always well understood. In particular, electronic interactions between the fullerene and the conjugated oligomer fragment have been stated for several dyads to explain their properties.^[3-4] However, unambiguous experimental evidence for such interactions is difficult to obtain, especially for hybrid systems in which the two components are separated by a flexible spacer. In order to clearly show the influence of π - π interactions between the conjugated system and the fullerene moiety on the electronic properties of C₆₀-(π -conjugated oligomer) dyads, we have designed compounds **1** and **2**. In both cases, by taking advantage of the peculiar structural features of macrocyclic fullerene bis adducts, the bridging π -conjugated oligomer unit and its fullerene partner are at the van der Waals contact (see Figure S1 in the Supporting Information). As a result, the absorption of the conjugated oligomer in **1** and **2** is dramatically red-shifted when compared to the corresponding model compounds lacking the fullerene subunit. In addition, the electronic coupling between the two terminal *N,N*-dimethylaniline redox centers is also influenced by the through-space intramolecular interactions of the C₆₀ units with the π -conjugated bridge.

[a] Laboratoire de Chimie des Matériaux Moléculaires, Université de Strasbourg et CNRS (UMR 7509), Ecole Européenne de Chimie, Polymères et Matériaux (ECPM), 25 rue Becquerel, 67087 Strasbourg Cedex 2, France
E-mail: nierengarten@chimie.u-strasbg.fr

[b] Institut de Ciència de Materials de Barcelona, Campus Universitari de Bellaterra and CIBER-BBN, Cerdanyola 08193, Spain
E-mail: cun@icmab.es
vecianaj@icmab.es

[c] Laboratoire de Chimie de Coordination du CNRS, 205 route de Narbonne, 31077 Toulouse Cedex 4, France
E-mail: beatrice.delavaux-nicot@lcc-toulouse.fr

Supporting information for this article is available on the WWW under <http://dx.doi.org/10.1002/ejoc.200900830>.

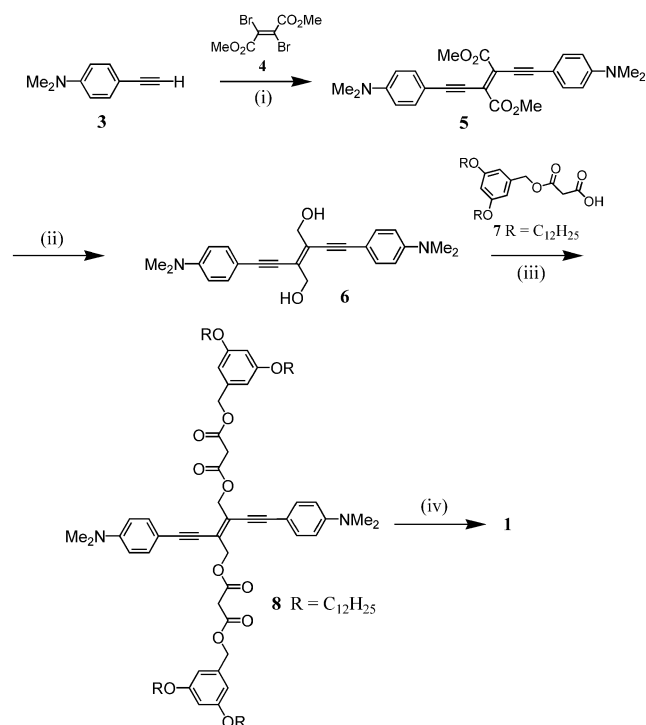


Results and Discussion

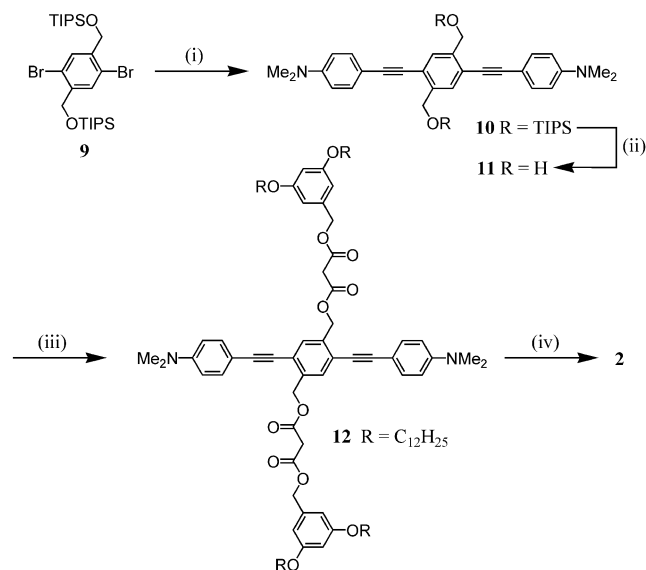
Synthesis

The synthesis of fullerene derivative **1** is depicted in Scheme 1. Compounds **3**^[5] and **4**^[6] were prepared according to previously reported procedures. Dimethyl 2,3-dibromofumarate (**4**) was subjected to a Pd-catalyzed cross-coupling reaction^[7] with 4-ethynyl-*N,N*-dimethylaniline (**3**) to give **5** in 79% yield. Subsequent treatment with diisobutylaluminum hydride (DIBAL-H) in CH₂Cl₂ afforded diol **6** in 69% yield. Reaction of **6** with carboxylic acid **7**^[8] under esterification conditions using *N,N'*-dicyclohexylcarbodiimide (DCC), 4-(dimethylamino)pyridine (DMAP) and 1-hydroxybenzotriazole (HOBt) gave bis-malonate **8** in 91% yield. Finally, fullerene derivative **1** was prepared by a macrocyclization reaction at the C sphere with bis-malonate **8** under the reaction conditions developed in the group of Diederich.^[9] The C₁-symmetric *cis*-2 bis-adduct **1** was thus obtained in 19% yield.

Fullerene derivative **2** was prepared in 4 steps from building block **9**^[10] (Scheme 2). Pd-catalyzed cross-coupling reaction of terminal alkyne **3** with bis-bromide **9** gave **10** in a moderate yield (18%). Indeed, compound **9** was found to be poorly reactive under Sonogashira conditions, most probably due to negative steric effects resulting from the presence of the bulky CH₂OTIPS moieties in the *ortho* position of the reactive bromide groups. However, sufficient quantities of compound **10** were thus obtained and no particular efforts were made to improve its preparation. Treatment of **10** with tetra-*n*-butylammonium fluoride (TBAF) in THF at 0 °C afforded compound **11** in a quantitative yield. Esterification of diol **11** with carboxylic acid **7** in the presence of DCC, HOBt and DMAP yielded bis-malonate **12** (92%) from which the C₁-symmetrical *trans*-4 bis-adduct **2** was obtained in 38% yield by macrocyclization with C₆₀.



Scheme 1. Reagents and conditions: (i) PdCl₂(PPh₃)₂, CuI, Et₃N, room temp. (79%); (ii) DIBAL-H, CH₂Cl₂, 0 °C (69%); (iii) DCC, DMAP, HOBt, CH₂Cl₂, 0 °C to room temp. (91%); (iv) C₆₀, DBU, I₂, PhMe, room temp. (19%).

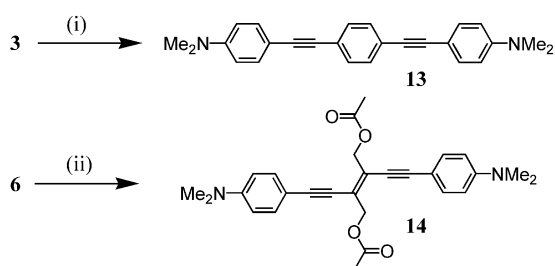


Scheme 2. Reagents and conditions: (i) **3**, PdCl₂(PPh₃)₂, CuI, PPh₃, THF, Et₃N, 65 °C (18%); (ii) TBAF, THF, 0 °C (99%); (iii) **7**, DCC, DMAP, HOBt, CH₂Cl₂, 0 °C to room temp. (92%); (iv) C₆₀, DBU, I₂, PhMe, room temp. (38%).

The structure and purity of compounds **1** and **2** were confirmed by ¹H and ¹³C NMR spectroscopy, mass spectrometry and elemental analysis. For both macrocyclic bis adducts **1** and **2**, the relative position of the two cyclopropane rings on the C₆₀ core (*cis*-2 for **1** and *trans*-4 for **2**) was determined based on the molecular symmetry (C₁ in both

cases) deduced from their ^1H and ^{13}C NMR spectra. In both cases, the proposed addition pattern on the fullerene sphere is also in perfect agreement with the one of previously reported fullerene bis adducts resulting from macrocyclization reactions of C_{60} with analogous tethered bis-malonates.^[9]

Finally, reference compounds **13** and **14** were prepared as shown in Scheme 3. Oligophenylene-ethynylene (OPE) derivative **13** was obtained in 77% from **3** and 1,4-diiodobenzene as described in the literature.^[11] DCC-Mediated esterification of diol **6** with AcOH afforded **14** in 82% yield as a crystalline orange solid. Crystals suitable for X-ray crystal-structure analysis were obtained by slow diffusion of hexane into a CHCl_3 solution of **14**. As shown in Figure 1, X-ray crystallography unambiguously confirmed the *E*-configuration of the alkene fragment in **14** and the N(1)–



Scheme 3. Reagents and conditions: (i) 1,4-diiodobenzene, $\text{PdCl}_2(\text{PPh}_3)_2$, CuI , Et_3N , room temp. (77%); (ii) AcOH, DCC, DMAP, HOBT, CH_2Cl_2 , 0 °C to room temp. (82%).

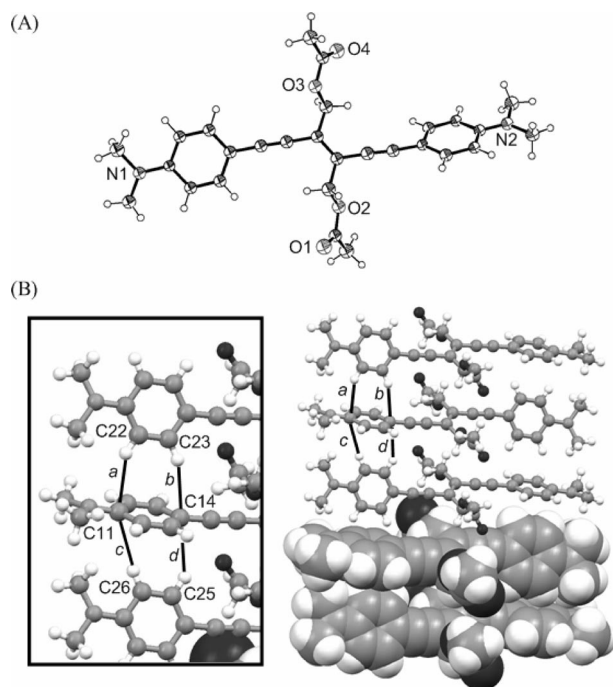


Figure 1. (A) ORTEP plot of the structure of **14** (thermal ellipsoids are drawn at the 50% probability level). (B) Stacking within the **14** lattice (view down the crystallographic axis *b*) highlighting the edge-to-face π - π interactions [a: C(22)H–C(11) 2.824 Å; b: C(23)H–C(14) 2.864 Å; c: C(26)H–C(11) 3.055 Å; d: C(25)H–C(14) 2.943 Å].

N(2) distance was found to be 17.245 Å. The conjugated diethynylethene backbone of **14** is nearly perfectly planar but dihedral angles of ca. 19.7° [Ar–N(1)] and 42.9° [Ar–N(2)] are observed for both terminal aromatic rings with respect to the diethynylethene plane. The peculiar orientation of these aromatic subunits can be explained by close inspection of the packing. Indeed, this orientation allows the establishment of intermolecular edge-to-face π - π interactions between the neighboring *para*-disubstituted phenyl rings (Figure 1, B). Observation of the crystal lattice down the crystallographic axis *b* reveals a layered structure in which the conjugated backbone of the molecules is aligned with axis *c*. Indeed, the **14** molecules are organized in columnar arrays parallel to the crystallographic axis *a* (Figure 1, B). In this way, simultaneous intermolecular edge-to-face π - π interactions of both phenyl units of **14** are possible with the two aromatic rings of both neighboring **14** molecules. Finally, it can be added that the aromatic rings of **14** giving rise to this intermolecular stacking are themselves in π - π interactions in a face-to-edge manner with molecules belonging to neighboring parallel columns (not shown).

Electronic Absorption Spectra

The absorption properties of compounds **1**, **2**, and of their reference compounds **14** and **13** were investigated in three different solvents, namely toluene, CH_2Cl_2 and THF. As typical examples, the absorption spectra recorded for all the compounds in CH_2Cl_2 solutions are reported in Figure 2. The UV/Vis spectra obtained for all compounds show a strong absorption with a maximum between 360 and 440 nm which is assigned to the π - π^* electronic transition of the conjugated system. For both **1** and **2**, the additional intense bands observed in the UV and the much weaker features seen in the visible spectral region correspond to the characteristic absorption of the fullerene chromophore.

Interestingly, the characteristic π - π^* electronic transition band of the conjugated system is significantly red-shifted in **1** with respect to model compounds **14** ($\Delta\lambda_{\text{max}} = 34$ nm in CH_2Cl_2). This red-shift between **1** and **14** was observed in all the investigated solvents and found to be concentration independent in the typical range for spectroscopic measurements, i.e. 10^{-7} – 10^{-5} M. Therefore it is only attributable to through space *intramolecular* interactions occurring between the fullerene sphere and its bridging diethynylethene unit. Importantly, the absorption spectrum of the C_{60} -OPE conjugate **2**, relative to reference compound **13**, shows the same trend (Figure 2). As a result of the substantial ground state interactions between the fullerene and the π -conjugated bridge, the absorption maximum of the OPE fragment is bathochromically shifted by ca. 24 nm in **2** when compared to reference compound **13**. For both **1** and **2**, the HOMO–LUMO gap of the conjugated system is affected by the π - π interactions with its neighboring electron-withdrawing C_{60} unit. It is worth mentioning that red-shifts have been reported for the porphyrin absorption in covalent and

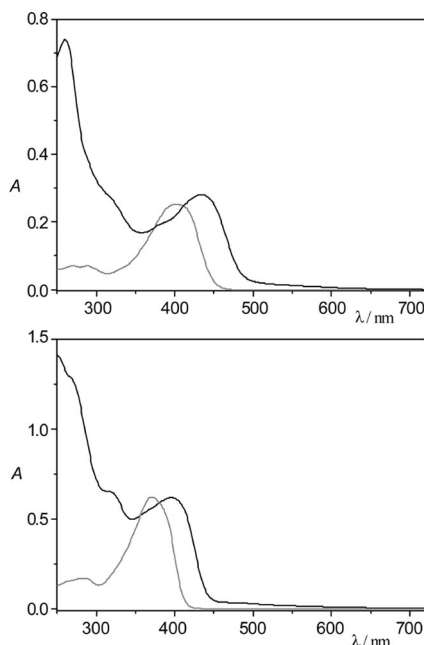


Figure 2. Top: absorption spectra of **1** (black) and **14** (gray) in CH_2Cl_2 at 298 K. Bottom: absorption spectra of **2** (black) and **13** (gray) in CH_2Cl_2 at 298 K.

non-covalent C_{60} -porphyrin conjugates as a result of intramolecular π -stacking interactions between the two chromophores.^[12–13] Similar effects have also been described for supramolecular complexes obtained from extended tetrathiafulvalene (ex-TTF) derivatives and C_{60} .^[14] It appears that the characteristic signature of π - π interactions of the fullerene unit with donors is a significant bathochromic shift of the absorption bands of the donor moiety.

Electrochemical Properties

The electrochemical properties of compounds **1**, **2**, **13**, and **14** were investigated by cyclic voltammetry (CV). The experiments were performed at room temperature in THF/nitrobenzene (9:1) solutions containing tetra-*n*-butylammonium hexafluorophosphate (0.1 M) as supporting electrolyte. Potential data for all of the compounds are collected in Table 1.

Table 1. Electrochemical properties of **1**, **2**, **13**, and **14** determined by cyclic voltammetry on a Pt working electrode in THF/nitrobenzene (9:1) with 0.1 M $[(n\text{Bu}_4)\text{N}]\text{PF}_6$ at room temp.

Compound	Reduction	Oxidation	E_{pa}
	$E_{1/2}$	$E_{1/2}$	
14		+0.35 ^[a,b]	
1	−1.09 ^[a]	+0.38 ^[a,b]	
13			+0.38 ^[b,c]
2	−1.09 ^[a]		+0.42 ^[b,c]

[a] Values for $(E_{pa} + E_{pc})/2$ in V vs. Fc/Fc^+ at a scan rate of 0.1 V s^{-1} . [b] Bielectronic process. [c] Irreversible process, E_p value in V vs. Fc/Fc^+ at a scan rate of 0.1 V s^{-1} .

In the cathodic region, **1** and **2** give rise to a reduction wave at -1.09 V vs. Fc/Fc^+ corresponding to the first reduction of the fullerene. When compared to related fullerene bis adducts,^[15] the redox potential values obtained for **1** and **2** are only weakly affected by the intramolecular π - π interactions between the fullerene moiety and the π -conjugated oligomer. This is in line with previous observation on C_{60} -porphyrin conjugates for which the redox potentials of the fullerene-centered reductions are almost not affected by its interaction with the porphyrin unit.^[12] In the anodic scan, all compounds show a two-electron process attributed to the simultaneous oxidation of the two *N,N*-dimethylaniline units suggesting weak electronic interactions between the two redox centers. While the oxidation of the bis(dimethylamino)-OPE derivatives **2** and **13** is irreversible, the oxidation process is reversible for **1** and **14** under these conditions. Comparison of the oxidation potential of the *N,N*-dimethylaniline moieties in **14** and **13** with those obtained for **1** and **2** shows only a very weak effect of the fullerene moieties ($\Delta E = 30\text{--}40 \text{ mV}$). Indeed, the oxidation process does not directly involve the conjugated system but mainly takes place on the N atoms of the terminal aniline subunits for which no specific through-space intramolecular π - π interactions with the C_{60} units are possible. For this reason, the oxidation of the aniline groups is only weakly affected by the electronic interactions between the conjugated bridging system and the accepting C_{60} spheroid. However, these intramolecular interactions should modulate the ability of the π -conjugated bridge to carry one electron from one aniline redox unit to the other in the mono-oxidized compounds derived from **1** and **2** as already demonstrated for fullerene-substituted mixed-valence bis(ferrocenylethynyl) ethene derivatives.^[16] Disappointingly, all attempts to perform stepwise coulometric titration with **1**, **2**, **13**, and **14** failed due to the instability of the oxidized species.^[17–18] Fortunately, oxidized species derived from compounds **1** and **14** could be generated chemically in THF/nitrobenzene (9:1) by addition of $\text{Fe}(\text{ClO}_4)_3$. Their formation was followed by absorption spectroscopy. Owing to the poor stability of the oxidized species, it was necessary to add increasing amounts of $\text{Fe}(\text{ClO}_4)_3$ to fresh solutions every time, and to work under strictly anhydrous conditions and under argon. The evolution of the UV/Vis/NIR spectra of compounds **1** and **14** during the chemical oxidation process is shown in Figure 3.

During the oxidation process of compounds **1** and **14** the amine bands around 400 and 450 nm disappear and new bands appear. The appearing band at 645 nm for **14** and the shoulder at 604 for **1** increases upon increase of the oxidant concentration and are assigned to the radical cation of the amine.^[18] More interesting is the weak and broad band centered at 1626 and 1300 nm, for **1** and **14**, respectively, that appears and increases continuously until complete formation of their mixed-valence compounds. Afterwards, the intensity of this band decreases until it disappears when the dicationic species **12**²⁺ and **14**²⁺ are completely formed. This behavior is typical of an intervalence charge-

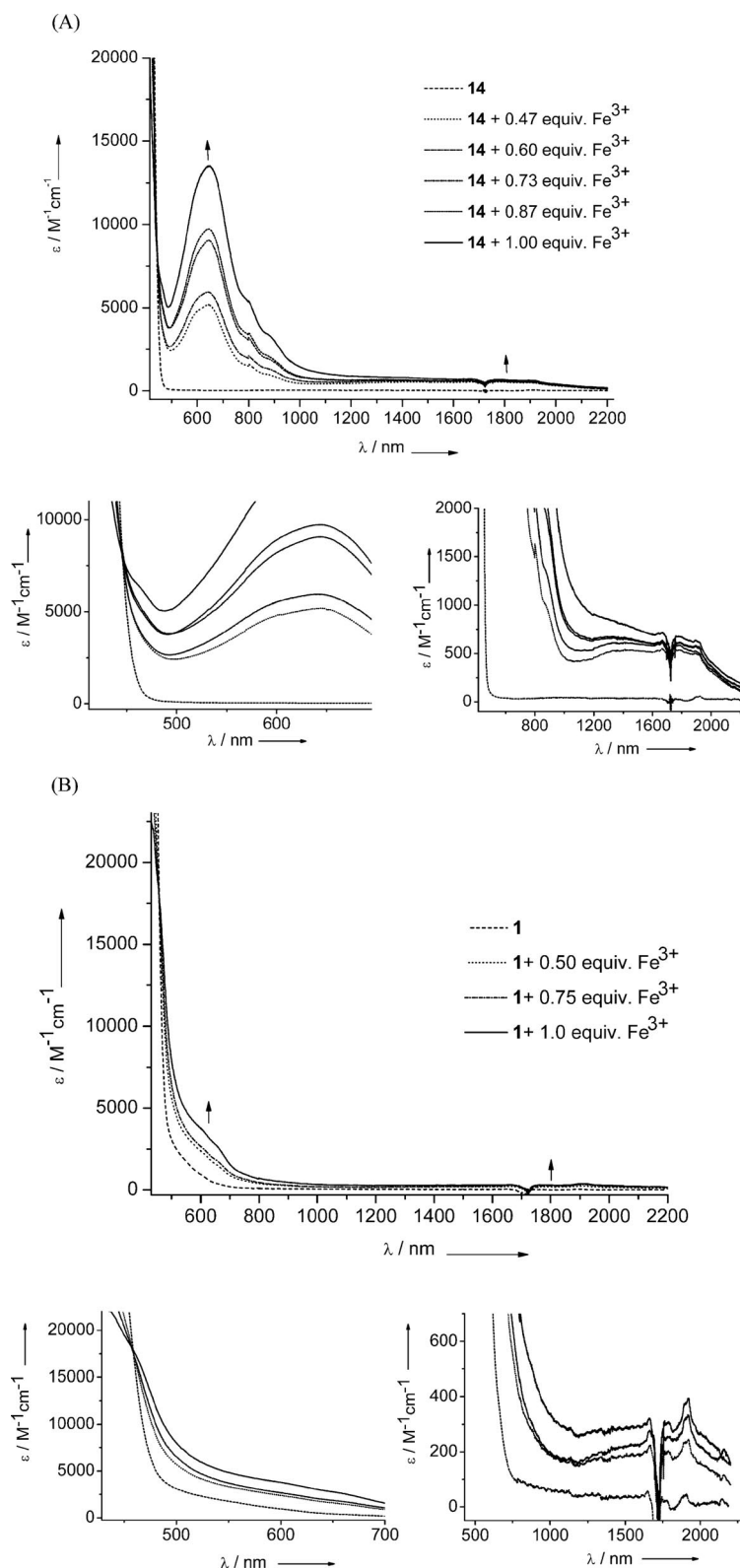


Figure 3. (A) Top: evolution of the UV/Vis/NIR spectra of compound **14** in THF/nitrobenzene (9:1) during the chemical oxidation process by addition of increasing amounts of $\text{Fe}(\text{ClO}_4)_3$ in a fresh solution of **14** every time. Bottom, left: expanded spectra of the visible region showing an isosbestic point. Bottom right: expanded spectra of the NIR region showing the increase of the intramolecular electron transfer absorption band until the maximum when the mixed-valence species is completely formed. (B) Top: evolution of the UV/Vis/NIR spectra of compound **1** in THF/nitrobenzene (9:1) during the chemical oxidation process by addition of increasing amounts of $\text{Fe}(\text{ClO}_4)_3$ in a fresh solution of **1** every time. Bottom, left: expanded spectra of the visible region showing an isosbestic point. Bottom, right: expanded spectra of the NIR region showing the increase of the intramolecular electron-transfer absorption band until a maximum when the mixed-valence species is completely formed.

transfer (IV-CT) band due to the presence of an intramolecular electron-transfer process in a Class II mixed-valence compound.^[19]

Along with the changes of these bands, the appearance and maintenance of one well-defined isosbestic point for both **1** (at 458 nm) and **14** (at 445 nm) indicates that in the used experimental conditions the formed mixed-valence species do not decompose (Figure 3).

From the characteristics of the IV-CT band, the effective electronic coupling V_{ab} (in cm^{-1}) between both aniline redox centers can be determined, using Equation (1) developed by Hush.^[20]

$$V_{ab} = \left[2.05 \times 10^{-2} \sqrt{\varepsilon_{\max} \tilde{\nu}_{\max} \Delta\nu_{1/2}} \right] R^{-1} \quad (1)$$

In this equation $\Delta\nu_{1/2}$ (in cm^{-1}) is the half-height band width of the IVCT band, R (in Å units) is the distance between the redox centres (here the distance between the two nitrogen atoms, as determined by the X-ray structure of **14**), ε_{\max} (in $\text{M}^{-1} \text{cm}^{-1}$) is the maximum molar extinction coefficient, and $\tilde{\nu}_{\max}$ (in cm^{-1}) the wavenumber at the maximal absorbance. Equation (1) gives an effective electronic coupling (V_{ab}) of 152 cm^{-1} for **1**⁺, and 291 cm^{-1} for **14**⁺ taking into account the comproportionation constants to recalculate the molar extinction coefficient. The spectroscopic data of IV-CT bands obtained from the deconvolution (see Figures S2 and S3, Supporting Information) of the experimental spectra of **1**⁺ and **14**⁺ are summarized in Table 2.

Table 2. Spectral data of the IV-CT bands obtained from the deconvolution of the experimental spectra of **1**⁺ and **14**⁺ and calculated V_{ab} values.

	$\nu_{\max} / \text{cm}^{-1}$	$\varepsilon_{\max} / \text{M}^{-1} \text{cm}^{-1}$	$\Delta\nu_{1/2} / \text{cm}^{-1}$	$R_{\text{N-N}} / \text{Å}$	V_{ab} / cm^{-1}
14 ⁺	7700	1700	4592	17.245	291
1 ⁺	6150	592	4468	17.245	152

The effective electronic coupling (V_{ab}) value for **14**⁺ is almost double the one found for **1**⁺ indicating that the electronic interactions between the two redox centres linked with the same conjugated bridge are different. This behaviour is accounted for the through space intramolecular interaction between the π -conjugated bridge and the C_{60} unit that generates an electrostatic field able to affect the HOMO–LUMO gap of the conjugated wire.

Conclusions

Two macrocyclic dyads combining C_{60} with π -conjugated oligomers have been prepared. Owing to their cyclic structure, the fullerene moiety and the π -conjugated oligomer substituent are forced to be at the van der Waals contact in both multicomponent systems. As a result, dramatic changes are observed in the absorption properties of both dyads. In particular, the absorption of the conjugated oligomer moiety is significantly red-shifted when compared to the corresponding model compounds lacking the fullerene

subunit. In contrast, cyclic voltammetry studies revealed that the changes in redox potentials of one component due to the presence of the other one are small. Even if the oxidation of the aniline groups is weakly affected by the electronic interactions between the conjugated bridging system and the fullerene moiety, these intramolecular interactions have a significant influence on the electronic coupling of the two aniline redox units in dyad **1**. Actually, when compared to model compound **14**⁺, delocalization of the positive charge in **1**⁺ is made more difficult by the π - π interactions of the conjugated system with the electron-withdrawing fullerene group. In conclusion, we have clearly shown that the existence of π - π interactions between the two components in C_{60} -(π -conjugated oligomer) dyads can be easily demonstrated by a significant bathochromic shift of the absorption bands of the conjugated system. Changes in redox potential are, however, quite weak, thus electrochemical data must be considered with care to demonstrate the occurrence of electronic interactions in such systems.

Experimental Section

General: Reagents and solvents were purchased as reagent grade and used without further purification. Compounds **3**,^[5] **4**,^[6] **7**,^[8] **9**,^[10] and **13**^[11] were prepared according to the literature. THF was distilled from sodium benzophenone ketyl. All reactions were performed in standard glassware under an inert Ar atmosphere. Evaporation and concentration were done at water aspirator pressure and drying in vacuo at 10^{-2} Torr. Column chromatography: silica gel 60 (230–400 mesh, 0.040–0.063 mm) was purchased from E. Merck and treated with Et_3N (1% in CH_2Cl_2) for the purification of compounds bearing NEt_2 groups. Thin-layer chromatography (TLC) was performed on glass sheets coated with silica gel 60 F_{254} purchased from E. Merck, visualization by UV light. IR spectra (cm^{-1}) were measured on an ATI Mattson Genesis Series FTIR instrument. NMR spectra were recorded on a Bruker AC 300 with solvent peaks as reference. UV/Vis/NIR spectra were taken on a Varian Cary 5 E spectrophotometer. MALDI-TOF-mass spectra were carried out on a Bruker BIFLEXTM matrix-assisted laser desorption time-of-flight mass spectrometer equipped with SCOUTTM High Resolution Optics, an X-Y multi-sample probe and a gridless reflector. Ionization is accomplished with the 337 nm beam from a nitrogen laser with a repetition rate of 3 Hz. All data were acquired at a maximum accelerating potential of 20 kV in the linear positive ion mode. The output signal from the detector was digitized at a sampling rate of 1 GHz. A saturated solution of 1,8,9-trihydroxyanthracene (dithranol from Aldrich, EC: 214-538-0) in CH_2Cl_2 was used as a matrix. Typically, a 1:1 mixture of the sample solution in CH_2Cl_2 was mixed with the matrix solution and 0.5 μL of the resulting mixture was deposited on the probe tip.^[21] Elemental analyses were performed by the analytical service at the Institut Charles Sadron, Strasbourg. The cyclic voltammetric measurements were performed on a 263A of EG&PAR potentiostat-galvanostat. Electrochemical experiments were performed in a conventional three-electrode cell consisting of platinum working and auxiliary electrodes and a Ag/AgNO_3 reference electrode. The experiments were carried out in ca. 10^{-3} M solution of samples in THF/nitrobenzene (9:1) containing 0.1 M $[(n\text{Bu}_4)\text{N}]\text{PF}_6$ (Fluka, $\geq 99\%$ electrochemical grade) as supporting electrolyte. Before each measurement, the solutions were degassed by bubbling argon for at least 5 min and the working electrode was burned to clean it. The

cyclic voltammograms were recorded under argon, at room temperature at a scan rate of 0.1 V s⁻¹. Under these experimental conditions, Fc⁺/Fc is observed at 0.58 V vs. Ag/AgNO₃.

Compound 5: A mixture of **3** (0.6 g, 4.15 mmol), **4** (0.5 g, 1.66 mmol), PdCl₂(PPh₃)₂ (280 mg, 0.39 mmol) and CuI (150 g, 0.79 mmol) in dry Et₃N (10 mL) was stirred at room temperature under argon for 12 h. The solution was concentrated, taken up in CH₂Cl₂ and filtered through a Celite pad. The organic phase was washed with H₂O, dried with MgSO₄ filtered and the solvents evaporated to dryness. Column chromatography (SiO₂, CH₂Cl₂/hexane, 7:3) yielded **5** (0.56 g, 79%). Dark red powder. ¹H NMR (300 MHz, CDCl₃): δ = 7.39 (d, *J* = 7 Hz, 4 H, Ar-H), 6.62 (d, *J* = 7 Hz, 4 H, Ar-H), 3.91 (s, 6 H, OCH₃), 3.00 [s, 12 H, N(CH₃)₂] ppm. C₂₆H₂₆N₂O₄ (430.50): calcd. C 72.54, H 6.09, N 6.51; found C 72.50, H 6.22, N 6.30.

Compound 6: A 1.0 M solution of DIBAL-H in hexane (1.8 mL, 1.8 mmol) was slowly added to a solution of **5** (150 mg, 0.35 mmol) in CH₂Cl₂ (5 mL) at 0 °C. The resulting mixture was stirred for 2 h. After 4 h, MeOH was added, then water. The resulting mixture was filtered through Celite and the solvents evaporated. Recrystallization from CH₂Cl₂/MeOH yielded **6** (90 mg, 69%). Orange powder. ¹H NMR (300 MHz, CDCl₃): δ = 7.34 (d, *J* = 7 Hz, 4 H, Ar-H), 6.66 (d, *J* = 7 Hz, 4 H, Ar-H), 4.55 (s, 4 H, CH₂), 3.00 [s, 12 H, N(CH₃)₂] ppm. C₂₄H₂₆O₂N₂ (374.48).

Compound 8: DCC (0.18 g, 0.89 mmol) was added to a solution of **6** (0.14 g, 0.37 mmol), **7** (0.53 g, 0.93 mmol), HOBT (23 mg, 0.15 mmol) and DMAP (18 mg, 0.15 mmol) in CH₂Cl₂ (15 mL) at 0 °C. After 1 h, the mixture was allowed to slowly warm to room temperature. After 12 h, the mixture was filtered and the solvents evaporated. Column chromatography (SiO₂, CH₂Cl₂) yielded **8** (0.5 g, 91%). Orange glassy product. ¹H NMR (300 MHz, CDCl₃): δ = 7.30 (d, *J* = 7 Hz, 4 H, Ar-H), 6.58 (d, *J* = 7 Hz, 4 H, Ar-H), 6.45 (d, *J* = 2 Hz, 4 H, Ar-H), 6.38 (t, *J* = 2 Hz, 2 H, Ar-H), 5.12 (s, 4 H, Ar-CH₂), 5.07 (s, 4 H, C=C-CH₂), 3.90 (t, *J* = 6 Hz, 8 H, OCH₂), 3.52 [s, 4 H, CH₂(C=O)₂], 2.97 [s, 12 H, N(CH₃)₂], 1.73 (m, 8 H, OCH₂CH₂), 1.50–1.26 (m, 72 H, CH₂), 0.87 (t, *J* = 7 Hz, 12 H, CH₂CH₃) ppm. ¹³C NMR (75 MHz, CDCl₃): δ = 166.2, 160.4, 137.3, 132.9, 111.9, 106.3, 101.2, 68.1, 67.2, 65.3, 41.4, 40.2, 31.9, 29.7, 29.65, 29.6, 29.55, 29.4, 29.3, 29.25, 26.0, 22.7, 14.1 ppm. C₉₂H₁₃₈N₂O₁₂ (1464.11): calcd. C 75.47, H 9.50, N 1.91; found C 75.66, H 9.66, N 1.90.

Compound 1: DBU (0.21 mL, 1.36 mmol) was added to a solution of C₆₀ (0.25 g, 0.34 mmol), I₂ (0.19 g, 0.75 mmol) and **8** (0.5 g, 0.34 mmol) in toluene (500 mL) at room temperature under argon. The solution was stirred for 12 h, filtered through a short plug of SiO₂ and concentrated. Column chromatography (SiO₂, CH₂Cl₂/hexane, 1:1) followed by gel permeation chromatography (Biorad, Biobeads SX1, CH₂Cl₂) gave **1** (0.14 g, 19%). Brown glassy product. ¹H NMR (300 MHz, CDCl₃): δ = 7.51 (d, *J* = 7 Hz, 2 H, Ar-H), 7.37 (d, *J* = 7 Hz, 2 H, Ar-H), 6.67 (d, *J* = 7 Hz, 2 H, Ar-H), 6.47 (d, *J* = 7 Hz, 2 H, Ar-H), 6.45 (d, *J* = 2 Hz, 2 H, Ar-H), 6.41 (d, *J* = 2 Hz, 2 H, Ar-H), 6.35 (t, *J* = 2 Hz, 1 H, Ar-H), 6.29 (t, *J* = 2 Hz, 1 H, Ar-H), 6.18 (d, *J* = 11 Hz, 1 H, C=C-CH), 5.55 (d, *J* = 11 Hz, 1 H, C=C-CH), 5.33 (d, *J* = 11 Hz, 1 H, Ar-CH), 5.27 (AB, *J* = 11 Hz, 2 H, Ar-CH₂), 5.11 (d, *J* = 11 Hz, 1 H, Ar-CH), 4.75 (d, *J* = 11 Hz, 1 H, C=C-CH), 3.83 (m, 8 H, OCH₂), 3.02 [s, 6 H, N(CH₃)₂], 2.89 [s, 6 H, N(CH₃)₂], 1.70 (m, 8 H, OCH₂CH₂), 1.50–1.26 (m, 72 H, CH₂), 0.88 (t, *J* = 7 Hz, 12 H, CH₂CH₃) ppm. ¹³C NMR (75 MHz, CDCl₃): δ = 162.8, 162.7, 162.5, 161.8, 160.35, 160.3, 150.8, 150.5, 148.9, 148.2, 147.4, 147.35, 147.25, 147.2, 145.9, 145.85, 145.8, 145.75, 145.65, 145.6, 145.5, 145.3, 145.3, 145.0, 144.95, 144.9, 144.85, 144.6, 144.55, 144.4, 144.1, 144.05,

144.0, 143.5, 143.4, 143.3, 143.0, 142.95, 142.9, 142.85, 142.8, 142.75, 142.3, 140.9, 140.0, 137.3, 136.9, 136.8, 136.75, 136.7, 136.1, 135.9, 135.4, 133.7, 133.3, 127.2, 126.9, 111.9, 111.7, 109.55, 109.5, 106.8, 106.7, 105.9, 104.5, 101.5, 101.4, 88.0, 86.3, 68.4, 68.3, 68.1, 68.0, 67.3, 67.0, 66.7, 66.6, 50.0, 49.7, 40.2, 40.1, 31.9, 29.7, 29.6, 29.45, 29.4, 29.3, 26.1, 22.7, 14.1 ppm. MALDI-TOF-MS: 2180.3 (M⁺, calcd. for C₁₅₂H₁₃₄O₁₂N₂: 2180.74). C₁₅₂H₁₃₄N₂O₁₂·CH₂Cl₂ (2265.68): calcd. C 81.11, H 6.05, N 1.24; found C 81.55, H 6.16, N 1.18.

Compound 10: As described for **5**, with **3** (0.2 g, 1.38 mmol), **9** (0.28 g, 0.46 mmol), PdCl₂(PPh₃)₂ (65 mg, 0.09 mmol), CuI (7 mg, 0.04 mmol) and PPh₃ (18 mg, 0.07 mmol) in THF/Et₃N (3:1) (4 mL). Two successive column chromatographies (SiO₂, CH₂Cl₂/hexane, 1:1) yielded **10** (0.06 g, 18%) as a yellow powder. ¹H NMR (300 MHz, CD₂Cl₂): δ = 7.68 (s, 2 H, Ar-H), 7.40 (d, *J* = 8 Hz, 4 H, Ar-H), 6.71 (d, *J* = 8 Hz, 4 H, Ar-H), 5.07 (s, 4 H, Ar-CH₂), 3.03 [s, 12 H, N(CH₃)₂], 1.18 [m, 42 H, Si(*i*Pr)₃] ppm. C₄₆H₆₈O₂N₂Si₂ (737.23).

Compound 11: A 1.0 M solution of TBAF in THF (0.25 mL, 0.25 mmol) was added to a stirred solution of **10** (0.06 g, 0.08 mmol) in THF (5 mL) at 0 °C under argon. After 4 h, the solution was concentrated and taken up in CH₂Cl₂. The organic layer was washed with H₂O, dried with MgSO₄, filtered and the solvents evaporated to dryness. Column chromatography (SiO₂, CH₂Cl₂) yielded **11** (34 mg, 99%) as a yellow powder. ¹H NMR (300 MHz, CD₂Cl₂): δ = 7.60 (s, 2 H, Ar-H), 7.43 (d, *J* = 8 Hz, 4 H, Ar-H), 6.71 (d, *J* = 8 Hz, 4 H, Ar-H), 4.89 (s, 4 H, Ar-CH₂), 3.03 [s, 12 H, N(CH₃)₂] ppm. C₂₈H₂₈O₂N₂ (424.54).

Compound 12: As described for **8**, with DCC (40 mg, 0.19 mmol), **11** (34 mg, 0.08 mmol), **7** (0.12 g, 0.2 mmol), HOBT (5 mg, 0.03 mmol) and DMAP (4 mg, 0.03 mmol) in CH₂Cl₂ (10 mL). Column chromatography (SiO₂, CH₂Cl₂) yielded **12** (0.11 g, 92%) as a yellow powder. ¹H NMR (300 MHz, CDCl₃): δ = 7.52 (s, 2 H, Ar-H), 7.38 (d, *J* = 8 Hz, 4 H, Ar-H), 6.63 (d, *J* = 8 Hz, 4 H, Ar-H), 6.45 (d, *J* = 2 Hz, 4 H, Ar-H), 6.38 (t, *J* = 2 Hz, 2 H, Ar-H), 5.40 (s, 4 H, Ar-CH₂), 5.10 (s, 4 H, Ar-CH₂), 3.88 (t, *J* = 6 Hz, 8 H, OCH₂), 3.52 [s, 4 H, CH₂(C=O)₂], 2.99 [s, 12 H, N(CH₃)₂], 1.75 (m, 8 H, OCH₂CH₂), 1.50–1.25 (m, 72 H, CH₂), 0.88 (t, *J* = 7 Hz, 12 H, CH₂CH₃) ppm. ¹³C NMR (75 MHz, CDCl₃): δ = 166.2, 166.2, 160.4, 150.3, 137.2, 135.9, 132.8, 131.2, 122.5, 111.7, 109.2, 106.2, 101.2, 97.9, 84.4, 68.0, 67.1, 65.2, 41.4, 40.1, 31.9, 29.6, 29.6, 29.4, 29.35, 29.2, 26.0, 22.7, 14.1 ppm. C₉₆H₁₄₀N₂O₁₂ (1514.17): calcd. C 76.15, H 9.32, N 1.85; found C 76.19, H 9.56, N 1.55.

Compound 2: As described for **1**, with C₆₀ (52 mg, 0.07 mmol), **12** (0.105 g, 0.07 mmol) DBU (0.05 mL, 0.28 mmol) and I₂ (39 mg, 0.15 mmol) in toluene (250 mL) Column chromatography (SiO₂, CH₂Cl₂/hexane, 1:1) followed by gel permeation chromatography (Biorad, Biobeads SX1, CH₂Cl₂) gave **2** (60 mg, 38%) as a brown glassy product. ¹H NMR (300 MHz, CDCl₃): δ = 7.61 (s, 1 H, Ar-H), 7.36 (d, *J* = 8 Hz, 2 H, Ar-H), 7.34 (s, 1 H, Ar-H), 7.32 (d, *J* = 8 Hz, 2 H, Ar-H), 6.63 (broad s, 4 H, Ar-H), 6.60 (d, *J* = 8 Hz, 2 H, Ar-H), 6.57 (d, *J* = 11 Hz, 1 H, Ar-CH), 6.54 (d, *J* = 8 Hz, 2 H, Ar-H), 6.46 (t, *J* = 2 Hz, 1 H, Ar-H), 6.45 (t, *J* = 2 Hz, 1 H, Ar-H), 5.91 (d, *J* = 11 Hz, 1 H, Ar-CH), 5.48 (d, *J* = 11 Hz, 1 H, Ar-CH), 5.46 (s, 2 H, Ar-CH₂), 5.44 (s, 2 H, Ar-CH₂), 4.98 (d, *J* = 11 Hz, 1 H, Ar-CH), 3.96 (t, *J* = 6 Hz, 4 H, OCH₂), 3.93 (t, *J* = 6 Hz, 4 H, OCH₂), 2.97 [s, 6 H, N(CH₃)₂], 2.95 [s, 6 H, N(CH₃)₂], 1.74 (m, 8 H, OCH₂CH₂), 1.50–1.24 (m, 72 H, CH₂), 0.87 (t, *J* = 7 Hz, 12 H, CH₂CH₃) ppm. ¹³C NMR (75 MHz, CDCl₃): δ = 164.2, 163.9, 163.85, 163.4, 160.5, 150.4, 150.35, 148.1, 146.9, 146.8, 146.7, 146.4, 146.3, 145.9, 145.8, 145.5, 145.4, 145.3, 145.25, 145.2, 145.1, 145.05, 145.0, 144.95, 144.7, 144.6, 144.5, 144.4,

144.3, 144.1, 143.9, 143.4, 143.0, 142.95, 142.9, 142.8, 142.75, 142.6, 142.5, 142.2, 142.1, 141.9, 141.85, 141.8, 141.7, 141.6, 141.4, 141.3, 141.2, 141.15, 141.1, 140.7, 140.3, 140.25, 139.7, 139.3, 136.7, 136.65, 136.4, 136.1, 134.9, 134.4, 132.9, 132.85, 132.7, 132.6, 132.2, 125.4, 124.6, 111.75, 111.7, 109.2, 109.15, 106.7, 106.3, 101.8, 101.7, 99.3, 98.2, 84.8, 84.4, 68.7, 68.6, 68.2, 68.14, 66.7, 66.1, 40.1, 31.9, 29.7, 29.6, 29.45, 29.35, 29.3, 26.1, 22.7, 14.2 ppm. MALDI-TOF-MS: 2230.6 (M^+ , calcd. for $C_{156}H_{136}O_{12}N_2$: 2230.80). $C_{156}H_{136}N_2O_{12}$ (2230.80): calcd. C 83.99, H 6.14, N 1.26; found C 83.70, H 6.36, N 1.19.

Compound 14: As described for **8**, with **6** (90 mg, 0.24 mmol), AcOH (0.04 mL, 0.6 mmol), DCC (0.12 g, 0.58 mmol), HOBT (15 mg, 0.1 mmol) and DMAP (12 mg, 0.1 mmol) in CH_2Cl_2 (10 mL). Column chromatography (SiO_2 , hexane/ CH_2Cl_2 , 1:1) yielded **14** (0.09 g, 82%) as orange crystals. 1H NMR (300 MHz, $CDCl_3$): δ = 7.32 (d, J = 8 Hz, 4 H, Ar-H), 6.62 (d, J = 8 Hz, 4 H, Ar-H), 5.05 (s, 4 H, CH_2), 2.99 [s, 12 H, $N(CH_3)_2$], 2.14 (s, 6 H, CH_3) ppm. ^{13}C NMR (75 MHz, $CDCl_3$): δ = 170.8, 150.4, 132.7, 125.3, 111.7, 109.2, 103.4, 84.3, 64.5, 40.1, 20.9 ppm. FAB-MS: 458.1 (M^+ , calcd. for $C_{28}H_{30}O_4N_2$: 458.22). $C_{28}H_{30}N_2O_4$ (458.56): calcd. C 73.34, H 6.59, N 6.11; found C 73.55, H 6.70, N 5.98.

X-Ray Crystal Structure of 14: Crystals suitable for X-ray crystal-structure analysis were obtained by slow diffusion of hexane into a CH_2Cl_2 solution of **14**. Data were collected at 180 K on an IPDS STOE diffractometer using a graphite-monochromated $Mo-K\alpha$ radiation (λ = 0.71073 Å) and equipped with an Oxford Cryosystems Cryostream Cooler Device. The structure was solved by direct methods using SIR92,^[22] and refined by means of least-squares procedures on F using the programs of the PC version of CRYSTALS.^[23] Atomic scattering factors were taken from the International Tables for X-ray Crystallography.^[24] Due to the lack of collected data, all atoms were refined with isotropic displacement parameters. Hydrogen atoms were located in a difference map, but those attached to carbon atoms were repositioned geometrically. All hydrogen atoms were refined using a riding model. $C_{28}H_{30}N_2O_4$ (M_r = 458.56), orange block crystal, 0.12 × 0.22 × 0.27 mm, triclinic, space group $P\bar{1}$, Z = 2, a = 9.5510(19) Å, b = 9.7090(19) Å, c = 13.529(3) Å, α = 86.47(3)°, β = 89.59(3)°, γ = 75.85(4)°, V = 1214.1(5) Å³, $\mu_{Mo-K\alpha}$ = 0.084 mm⁻¹. 12009 reflections were measured, 4439 unique (R_{int} = 0.06) and a total of 137 parameters was used. The final agreement factors were R = 0.0564, wR = 0.0544 for the 1508 reflections having $I > 3\sigma$.

CCDC-732861 contains the supplementary crystallographic data for this paper. These data can be obtained free of charge from The Cambridge Crystallographic Data Centre via www.ccdc.cam.ac.uk/data_request/cif.

Generation of Cation Radicals: Oxidized species derived from compounds **1** and **14** have been generated chemically in THF/nitrobenzene (9:1) by addition of $Fe(ClO_4)_3$. Their formation was followed by absorption spectroscopy. Owing to the poor stability of the oxidized species, it was necessary to add increasing amounts of $Fe(ClO_4)_3$ to fresh solutions every time, and work under strictly anhydrous conditions and under argon.

Supporting Information (see also the footnote on the first page of this article): Calculated structures of compounds **1** and **2**, and deconvolution of the NIR spectra of the mixed-valence species.

Acknowledgments

This research was supported by the Centre National de la Recherche Scientifique (CNRS) (UMR 7509), the Agence Nationale de

la Recherche (Solaire Photovoltaïque – Nanorgysol), the Spanish Dirección General de Investigación (DGI) (project EMOCIONa, CTQ2006-06333/BQU), the European Science Foundation (ESF) (EUROCORES-SONS “FUNSmarts II” project) and the Instituto de salud Carlos III, MIVC, through “Acciones CIBER”.

- [1] J. L. Segura, N. Martin, D. M. Guldi, *Chem. Soc. Rev.* **2005**, *34*, 31–47.
- [2] T. M. Figueira-Duarte, A. Gégout, J.-F. Nierengarten, *Chem. Commun.* **2007**, 109–119.
- [3] For selected examples, see: E. Peeters, P. A. van Hal, J. Knol, C. J. Brabec, N. S. Sariciftci, J. C. Hummelen, R. A. J. Janssen, *J. Phys. Chem. B* **2000**, *104*, 10174–10190; N. Armaroli, F. Barigelletti, P. Ceroni, J.-F. Eckert, J.-F. Nicoud, J.-F. Nierengarten, *Chem. Commun.* **2000**, 599–600; D. M. Guldi, C. Luo, A. Swartz, R. Gomez, J. L. Segura, N. Martin, C. Brabec, N. S. Sariciftci, *J. Org. Chem.* **2002**, *67*, 1141–1152; A. M. Ramos, S. C. J. Meskers, P. A. van Hal, J. Knol, J. C. Hummelen, R. A. J. Janssen, *J. Phys. Chem. A* **2003**, *107*, 9269–9283; M. Gutierrez-Nava, G. Accorsi, P. Masson, N. Armaroli, J.-F. Nierengarten, *Chem. Eur. J.* **2004**, *10*, 5076–5086; D. M. Guldi, C. Luo, A. Swartz, R. Gomez, J. L. Segura, N. Martin, *J. Phys. Chem. A* **2004**, *108*, 455–467.
- [4] J.-F. Eckert, J.-F. Nicoud, J.-F. Nierengarten, S.-G. Liu, L. Echegoyen, F. Barigelletti, N. Armaroli, L. Ouali, V. Krasnikov, G. Hadziioannou, *J. Am. Chem. Soc.* **2000**, *122*, 7467–7479.
- [5] M. Kivala, C. Boudon, J.-P. Gisselbrecht, P. Seiler, M. Gross, F. Diederich, *Chem. Commun.* **2007**, 4731–4733.
- [6] J. Anthony, A. M. Boldi, Y. Rubin, M. Hobi, V. Gramlich, C. B. Knobler, P. Seiler, F. Diederich, *Helv. Chim. Acta* **1995**, *78*, 13–45.
- [7] *Metal-catalyzed Cross-coupling Reactions* (Eds.: F. Diederich, P. J. Stang), Wiley-VCH, Weinheim, **1998**.
- [8] D. Felder, M. Gutiérrez Nava, M. del Pilar Carreon, J.-F. Eckert, M. Luccisano, C. Schall, P. Masson, J.-L. Gallani, B. Heinrich, D. Guillon, J.-F. Nierengarten, *Helv. Chim. Acta* **2002**, *85*, 288–319.
- [9] J.-F. Nierengarten, V. Gramlich, F. Cardullo, F. Diederich, *Angew. Chem. Int. Ed. Engl.* **1996**, *35*, 2101–2103; J.-F. Nierengarten, T. Habicher, R. Kessinger, F. Cardullo, F. Diederich, V. Gramlich, J.-P. Gisselbrecht, C. Boudon, M. Gross, *Helv. Chim. Acta* **1997**, *80*, 2238–2276; J.-F. Nierengarten, A. Herrmann, R. R. Tykwinski, M. Rüttimann, F. Diederich, C. Boudon, J.-P. Gisselbrecht, M. Gross, *Helv. Chim. Acta* **1997**, *80*, 293–316.
- [10] A. Gégout, M. Holler, T. M. Figueira-Duarte, J.-F. Nierengarten, *Eur. J. Org. Chem.* **2008**, 3627–3634.
- [11] P. Nguyen, Z. Yuan, L. Agocs, G. Lesly, T. B. Marder, *Inorg. Chim. Acta* **1994**, *220*, 289–296.
- [12] J.-P. Bourgeois, F. Diederich, L. Echegoyen, J.-F. Nierengarten, *Helv. Chim. Acta* **1998**, *81*, 1835–1844; J.-F. Nierengarten, C. Schall, J.-F. Nicoud, *Angew. Chem. Int. Ed.* **1998**, *37*, 1934–1936.
- [13] D. I. Schuster, P. D. Jarowski, A. N. Kirschner, S. R. Wilson, *J. Mater. Chem.* **2002**, *12*, 2041–2047; N. Armaroli, G. Marconi, L. Echegoyen, J.-P. Bourgeois, F. Diederich, *Chem. Eur. J.* **2000**, *6*, 1629–1645; N. Solladié, M. E. Walther, M. Gross, T. M. Figueira-Duarte, C. Bourgogne, J.-F. Nierengarten, *Chem. Commun.* **2003**, 2412–2413; N. Armaroli, G. Accorsi, F. Song, A. Palkar, L. Echegoyen, D. Bonifazi, F. Diederich, *ChemPhysChem* **2005**, *6*, 732–743; P. D. W. Boyd, C. A. Reed, *Acc. Chem. Res.* **2005**, *38*, 235–242, and references cited therein.
- [14] J. Santos, B. Grimm, B. M. Illescas, D. M. Guldi, N. Martin, *Chem. Commun.* **2008**, 5993–5995.
- [15] F. Cardullo, P. Seiler, L. Isaacs, J.-F. Nierengarten, R. F. Haldimann, F. Diederich, T. Mordasini-Denti, W. Thiel, C. Boudon, J.-P. Gisselbrecht, M. Gross, *Helv. Chim. Acta* **1997**, *80*, 343–371; Y. Rio, G. Enderlin, C. Bourgogne, J.-F. Nierengarten, J.-P. Gisselbrecht, M. Gross, G. Accorsi, N. Armaroli, *Inorg.*

- Chem.* **2003**, *42*, 8783–8793; U. Hahn, E. Maisonhaute, C. Amatore, J.-F. Nierengarten, *Angew. Chem. Int. Ed.* **2007**, *46*, 951–954; R. Pereira de Freitas, J. Iehl, B. Delavaux-Nicot, J.-F. Nierengarten, *Tetrahedron* **2008**, *64*, 11409–11419.
- [16] T. M. Figueira-Duarte, V. Lloveras, J. Vidal-Gancedo, A. Gégout, B. Delavaux-Nicot, R. Welter, J. Veciana, C. Rovira, J.-F. Nierengarten, *Chem. Commun.* **2007**, 4345–4347.
- [17] E. Ahlberg, B. Helgee, V. D. Parker, *Acta Chem. Scand., Ser. B* **1980**, *34*, 187–193.
- [18] S. Sumalekshmy, K. R. Gopidas, *Chem. Phys. Lett.* **2005**, *413*, 294–299.
- [19] M. Robin, P. Day, *Adv. Inorg. Radiochem.* **1967**, *10*, 247–422.
- [20] N. S. Hush, *Coord. Chem. Rev.* **1985**, *64*, 135–157; R. J. Cave, M. D. Newton, *J. Chem. Phys.* **1997**, *106*, 9213–9226.
- [21] Y. Rio, G. Accorsi, H. Nierengarten, J.-L. Rehspringer, B. Hönerlage, G. Kopitkovas, A. Chugreev, A. Van Dorsselaer, N. Armaroli, J.-F. Nierengarten, *New J. Chem.* **2002**, *26*, 1146–1154; Y. Rio, G. Accorsi, H. Nierengarten, C. Bourgogne, J.-M. Strub, A. Van Dorsselaer, N. Armaroli, J.-F. Nierengarten, *Tetrahedron* **2003**, *59*, 3833–3844; U. Hahn, M. Elhabiri, A. Trabolsi, H. Herschbach, E. Leize, A. Van Dorsselaer, A.-M. Albrecht-Gary, J.-F. Nierengarten, *Angew. Chem. Int. Ed.* **2005**, *44*, 5338–5341; J.-F. Nierengarten, U. Hahn, A. Trabolsi, H. Herschbach, F. Cardinali, M. Elhabiri, E. Leize, A. Van Dorsselaer, A.-M. Albrecht-Gary, *Chem. Eur. J.* **2006**, *12*, 3365–3373.
- [22] A. Altomare, G. Cascarano, C. Giacovazzo, A. Guagliardi, *J. Appl. Crystallogr.* **1993**, *26*, 343–350.
- [23] P. W. Betteridge, J. R. Carruthers, R. I. Cooper, K. Prout, D. J. Watkin, *J. Appl. Crystallogr.* **2003**, *36*, 1487.
- [24] *International Tables for X-ray Crystallography*, Kynoch Press, Birmingham, U.K., **1974**, vol. IV.

Received: July 23, 2009

Published Online: October 8, 2009